Drug Delivery

DOI: 10.1002/ange.201208077

Systemic Delivery of microRNA-34a for Cancer Stem Cell Therapy**

*Sanjun Shi, Lu Han, Tao Gong, Zhirong Zhang, and Xun Sun**

Although many potent conventional therapies are available to cancer patients, the spontaneous reappearance of tumors in the long term remains a significant concern with these therapies.[1] This unfortunate phenomenon of therapeutic relapse may be caused by the lack of efficiency in eliminating the cancer stem cell (CSC) population in the tumor mass. For example, lung cancer accounts for the majority of cancer-related deaths worldwide.[2] Currently, chemotherapy and radiotherapy remain the basis of treatment against lung cancer because of their capability to reduce the whole tumor bulk. However, such reduction is nonspecific with regard to CSCs, resulting in development of relapse and resistance to treatment. Thus, use of conventional therapies for the treatment of lung cancer is limited. CSC-specific targeting has been introduced as an alternative, because of its potential to kill tumor-initiating cancer cells.[3] The identification of CSC markers and their exploitation in targeted chemotherapy is an ultimate goal for CSC-based therapy.[4] Recently, CD44 has been demonstrated to serve as an important marker of a subset population of CSCs in many tumors, including lung cancer.[3] However, specific therapeutic targeting of CD44 in CSCs is still in its infancy.

MicroRNA-34a (miR-34a), which is one of the most prominent endogenous miRNAs involved in the genesis and progression of human cancers, functions as a tumor suppressor and is commonly down-regulated in many human cancers. Enhanced expression of miR-34a in the lung inhibits tumor growth, owing to the down-regulation of the protein survivin in the tumor.[5] Recently, miR-34a was reported to be an important regulator, inhibiting both CSC differentiation and metastasis by directly repressing the CSC marker CD44, suggesting that CD44 is a direct and functional target of miR-34a.[6] Thus, the involvement of miR-34a in suppressing CSC proliferation makes it a promising candidate for lung cancer therapy.

Nevertheless, the therapeutic effect of nuclease-labile and hydrophilic molecules such as miRNAs is hampered by poor delivery systems.[7] Therefore, it is important to develop an effective and functional drug-delivery system for miRNAs, which should have the two following key characteristics:[8] 1) it protects encapsulated miRNAs from degradation by nucleases when the nucleic acids circulate in the blood; 2) it includes a cationic component that facilitates association with anionic miRNAs. Additional properties that are more generally applicable to delivery systems would include, but are not necessarily limited to: outstanding cellular-uptake efficiency both in vitro and in vivo, and accumulation of the drug at the correct tumor site. To date, use of viral vectors for gene delivery may be accompanied by an immune response,[9] and direct evidence for the clinical applicability of polymer-based nanoparticles is still limited. To address these issues, solid lipid nanoparticles (SLNs) with the required properties (mentioned above) are beginning to emerge for delivery of many drugs, including gene-based drugs.[10] Additionally, it remains unclear how to properly and efficiently deliver CSC-modulating macromolecules, such as miR-34a, into the lung for CSC therapy.

In an effort to find an appropriate delivery method, we employed SLNs that contain dimethyldioctadecylammonium bromide (DDAB) to condense miRNAs in order to enhance cellular uptake and increase the localization of the drug in the cancerous lung, followed by repressing the CSC properties. The miSLNs-34a formulation (miR-34a-loaded DDAB-SLNs) was characterized, followed by in vitro and in vivo assessment of its enhanced stability and antitumor properties. Furthermore, the CD44 (CSC-like) phenotype was evaluated after intravenous injection of miSLNs-34a into B16F10-$CD44^+$-bearing tumors in mouse lungs. Taken together, miR-34a is considered a new functional regulator of CD44,[6] and to our knowledge, this is the first miR-34a delivery system to achieve efficient CSC therapy.

Herein, DDAB-containing solid lipid nanoparticles were prepared by a film-ultrasonic method (see Experimental Section in the Supporting Information). MiRNA-loaded SLNs (miSLNs) were then prepared by coincubation of SLNs with miRNA at different ratios (DDAB/RNA, *w*/*w*). Figure 1 and Figure S1 in the Supporting Information show the size distributions and morphology of SLNs and miSLNs. The average size of miSLNs, having spherical morphology, was approximately 200 nm, which is within the injectable range for intravenous administration ($\approx$200 nm).[11] The entrapment efficiency of miSLNs was $(96.44 \pm 0.17)\,\%$, and the RNA loading yield in miSLNs was (2.57 ± 0.10) nmol per mg of lipids. In addition, Table S1 shows that SLNs can protect miRNA from degradation, and this protection ability was better than that of lipofectamine.

We first determined the properties of B16F10-$CD44^+$ cells by sphere-formation assays in in vitro cellular studies and found that the B16F10-$CD44^+$ cells were CSC-like (Figure S2). An investigation of the cytotoxicity of the excipients

[*] S. J. Shi, L. Han, Prof. T. Gong, Prof. Z. R. Zhang, Prof. X. Sun
Key Laboratory of Drug Targeting and Drug Delivery Systems
Ministry of Education, West China School of Pharmacy
Sichuan University Chengdu
No.17, Section 3, Renmin South Rd, Chengdu, 610041 (P.R. China)
E-mail: xunsun22@gmail.com

[**] We thank the National Science Foundation of China (No. 81130060), the Program for New Century Excellent Talents in University (No. NTEC-10-0601), and the National Science & Technology Major Project of China (No. 2011ZX09401-304(4-3)) for financial support. We also thank Dr. Chester Provoda from the University of Michigan for his help in preparing this manuscript.

Supporting information for this article is available on the WWW under http://dx.doi.org/10.1002/anie.201208077.

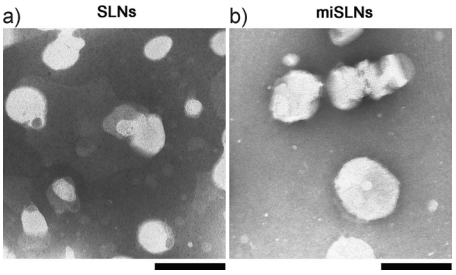

Figure 1. Blank SLNs (a) and miSLNs (b) visualized by transmission electron microscopy (TEM). Scale bar: 200 nm.

showed that SLNs were well tolerated (low toxicity) by B16F10-CD44$^+$ cells at lower concentrations (from 9–19 μg mL^{-1}) of DDAB in the nanoparticles (Figure S3). The cellular uptake of miSLNs-34a was then evaluated by flow cytometry and quantitative real-time PCR (qRT-PCR). Increasing the DDAB/RNA ratio to 8:1 (DDAB/RNA, *w*/*w*) resulted in enhanced cellular uptake of nanoparticles (Figure S4a), thus indicating that the positive charge of miSLNs could contribute to the cellular uptake of the particles.[12] However, a further increase of the ratio beyond 8:1 did not result in further enhanced cellular uptake. Therefore, in the following studies, the DDAB/RNA ratio was set at 8:1 (*w*/*w*), which showed the highest cellular-uptake efficiency. Then, expression of mature miR-34a was quantified at 24 h after transfection. Compared with untreated and miR-34a-treated groups, B16F10-CD44$^+$ cells transfected with miSLNs-34a had 297.1-fold and 90.7-fold higher miR-34a levels, respectively (Figure S4b). Additionally, compared to lipo-RNA, the uptake of miSLNs was slightly lower because of the blocking activity of polyoxyethylene 50 stearate (Myrj53) coated on the surface of nanoparticles.

The wound-healing assay provides a valuable in vitro tool for studying the combined processes of cell migration, cell motility, and proliferation.[13] B16F10-CD44$^+$ cells migrate faster into the scratch, and the recovery of the wound area was nearly completed within one day in groups treated with PBS, mock (all reagents except for miR-34a), free miR-34a, miSLNs-NC, and lipo-NC (NC: negative control oligonucleotide of miR-34a), while miSLNs-34a and lipo-miR-34a inhibited the wound closure of all scratches (see Figure 2a, and Figure S5 in the Supporting Information). These results also illustrate that miSLNs-34a-treated and lipo-miR-34a-treated tumor cells were attenuated in cell motility and migration, but other groups did not show this attenuation.

To investigate the influence of the miR-34a formulations on cell apoptosis, cell morphology changes were evaluated by DAPI staining and the number of apoptotic cells was quantified by annexin V-FITC and propidium iodide (PI) double-staining. Compared with the negative control groups, extreme chromatin condensation, nuclear fragmentation, and apoptotic body formation occurred in a substantially greater number of cells in both miSLNs-34a and lipo-miR-34a groups (see Figure 2b, and Figure S5b in the Supporting Information). Accordingly, miSLNs-34a and lipo-miR-34a could induce the death of B16F10-CD44$^+$ cells (Figure S6). Histograms in Figure 2c show that the lipo-miR-34a group had the highest fraction of cells (55.3%) in the annexin V$^+$/PI$^-$ (apoptotic) quadrant, while miSLNs-34a showed a slightly decreased fraction of apoptotic cell (47.6%), but displayed a greater percentage of cells in the annexin V$^+$/PI$^+$ (apoptotic and necrotic) quadrant (22.4%). This observation might be attributed to the excipient DDAB that was used, which is toxic to cells and can induce necrosis. In addition, the subpopulation of miSLNs-34a-induced apoptotic cells was a significantly greater frac-

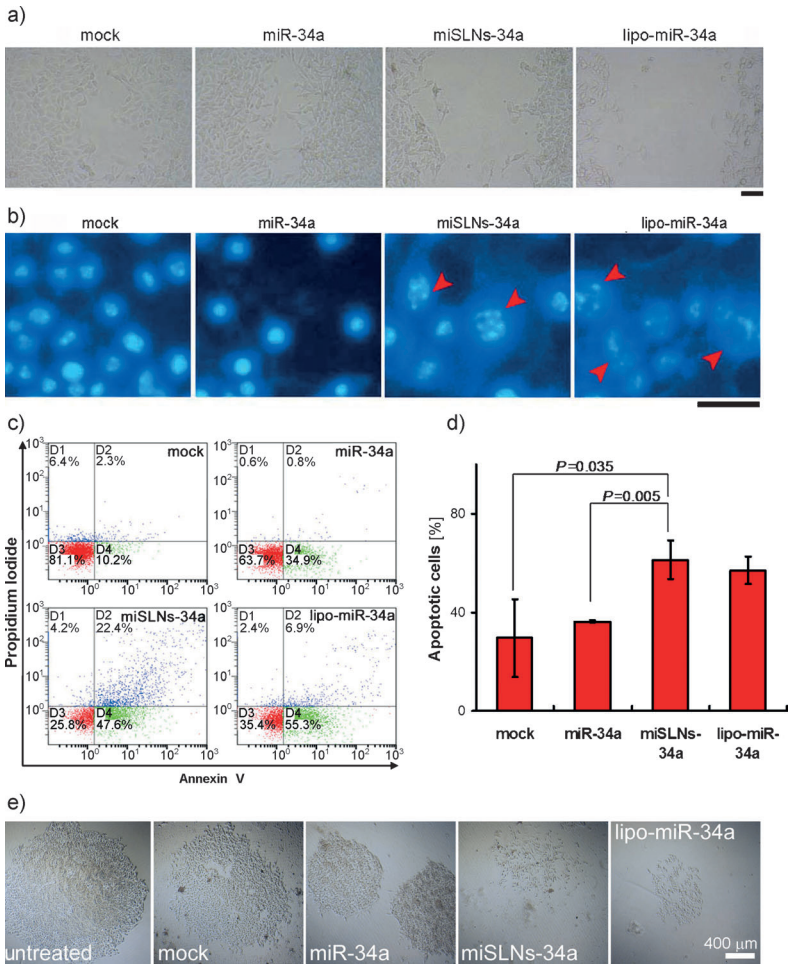

Figure 2. In vitro cellular evaluation of miSLNs. a) Effects of miSLNs-34a on B16F10-CD44$^+$ cell motility and migration: representative images of wound-healing assay. Scale bar: 30 μm. b) DAPI staining of fragmented chromatin or apoptotic bodies in B16F10-CD44$^+$ cells after transfection with miSLNs. Scale bar: 30 μm. c) Necrosis and apoptosis assays conducted by flow cytometry using Annexin V in combination with propidium iodide. d) Proportion of apoptotic cells after treating with miR-34a ($n=3$). e) Sphere-formation assays. Images were taken at 72 h after miSLN administration and representative spheres are shown.

tion than that of both mock and miR-34a groups ($P < 0.05$; Figure 2d).

Spheroid-colony formation, which is an in vitro cell-culture model to identify CSCs, is considered an indication of self-renewal ability and would be consistent with a CSC-like phenotype or property.[14] Untreated B16F10-CD44$^+$ cells successfully produced spheroid colonies (Figure 2e). Spheres treated with miR-34a delivered by miSLNs and lipofectamine showed a suppressive effect on the formation of sphere colonies. As expected, the other groups containing untreated, mock, and free miR-34a did not exhibit this effect (Figure 2e). These findings suggest that miSLNs-34a could greatly impact the ability of B16F10-CD44$^+$ cells to form CSC-like spheroids in vitro.

MiR-34a has been shown to influence the expression of CD44 on CSC-like cells[6] by functioning as a CSC marker,[6,14b] thus playing a role in tumor cell adhesion. Therefore, CD44-positive B16F10 cells were used as the CSC-like cell population to evaluate the function of miR-34a (against CD44) in different formulations. Using an anti-CD44 antibody for flow cytometry, relatively low CD44 expression was detected on the cell surface in miSLNs-34a and lipo-miR-34a treatment groups, as compared with the expression of CD44 in the control groups (Figure 3). The decrease in CD44 was miR-34a-dependent and was not observed with free miR-34a alone, indicating that lipo-miR-34a and miSLNs-34a were efficiently internalized into cells, but free miR-34a was not. These results demonstrated that miSLNs-34a could reduce expression of CD44, inhibit cell migration, and induce cell apoptosis (Figure 2). These observations are consistent with CD44 being a direct and functional target of miR-34a in CSCs,[6] and with CD44 possibly playing a role in mediating CSC migration, homing, and metastasis.[6,15] In those reports, all of these anti-CSC activities were well correlated with the high miR-34a expression levels in the cells. Thus, miR-34a delivery mediated by miSLNs is a promising strategy to attenuate CD44-positive CSC growth and migration.

The in vivo biodistribution characteristics of miSLNs were monitored using fluorescence imaging and qRT-PCR. Carboxyfluorescein-labeled SLNs accumulated in the lung, and a gradual increase in fluorescence signals was observed in the lungs from 1–2 h after intravenous injection, followed by a plateau in the signal intensity at 3 h (Figure 4a). Additionally, use of SLNs resulted in the intracellular and cytosolic delivery of the drug (fluorescence signals; Figure 4b). Then, in order to verify whether SLNs could deliver the model drug miR-34a into the lung, Cy3-miR-34a was loaded into nanoparticles for intravenous administration to the mice. The ex vivo tissues were collected for image monitoring (Figure 4c), showing that miSLNs could efficiently mediate miR-34a delivery into the lung, while lipofectamine was relatively inefficient. These results suggest that lipo-miR-34a was mainly taken up by reticuloendothelial system (RES) organs, such as the liver. However, DDAB-containing SLNs (zeta potential) and Myrj53 could induce the accumulation of SLNs in the lung (Figure S7). Accordingly, it is plausible that miSLNs-34a avoids unwanted liver capture because of the PEG-like structure of Myrj53 in the SLN shell, which considerably reduces the adsorption between nanoparticle and protein,[16] thereby prolonging its circulation time ($t_{1/2} =$ 8.16 h, Figure S8) and decreasing the uptake of SLNs by Kupffer cells. The qRT-PCR results (Figure 4d) show that the lungs treated with miSLNs-34a exhibited the highest miR-34a expression and a 5.9-fold greater miR-34a level relative to that of lipo-miR-34a-treated lung tissues. Taken together, these findings indicate that miSLNs enhance miR-34a uptake into the lung, primarily owing to the ability of the delivery vehicle to avoid liver capture and be physically entrapped in the capillary bed of the lungs.[17] Therefore, this observation indicates the feasibility of developing this strategy for lung

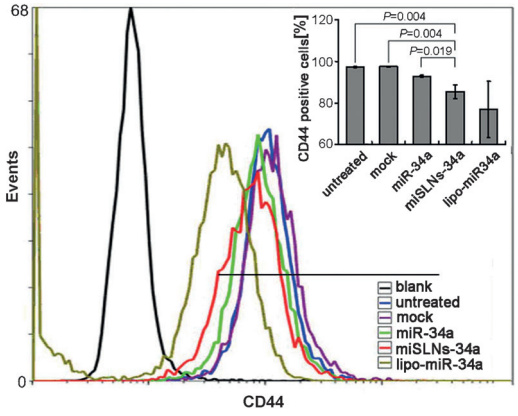

Figure 3. Flow cytometric evaluation of CD44 expression in the B16F10-CD44$^+$ cells after miR-34a treatments.

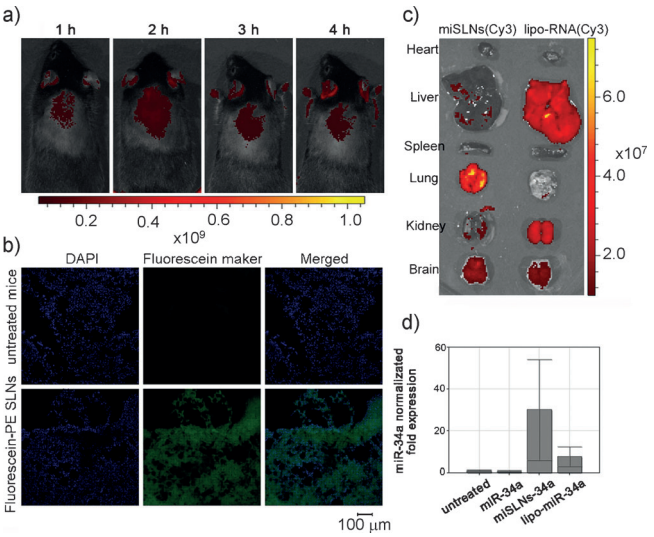

Figure 4. In vivo fluorescence images of miSLNs in mice and mature miR-34a levels in the lungs. a) Time-dependent intensity images of fluorescence distribution in mice. b) Fluorescence microscopy images of lung tissue sections at 2 h after intravenous injection of fluorescence-labeled SLNs (Blue fluorescence shows nuclear staining with DAPI, and green fluorescence shows the location of SLNs). c) In vivo fluorescence images of major organs at 2 h after injection of miSLNs. d) Mature miR-34a levels in lung tissues 24 h after mice were given intravenous injections with miSLNs ($n = 5$).

cancer therapy by using the miSLNs approach to deliver miR-34a. In addition, based on the biodistribution of the lipofectamine group, the lipo-miR-34a preparation was not further investigated in the remaining in vivo studies.

Aiming to verify whether miSLNs-34a had antitumor efficacy in the CSC-bearing mice, their survival rates, along with the weight and histological staining of lungs and CD44 expression, were analyzed. As expected, the mice in the control groups, which were treated with PBS, mock, and miR-34a, died relatively quickly, while miSLNs-34a significantly prolonged the survival time of mice (Figure 5a). Histological analysis of the tumor by hematoxylin and eosin (H&E) staining as well as the lung morphology showed that the growth of the tumor nodules in the lung was significantly inhibited by miSLNs-34a, as compared with other control groups (Figure 5b,c). Notably, significant decreases in the weights of CSC-like B16F10-bearing lungs were found in the miSLNs-34a group compared with the groups that were treated differently ($P<0.05$; Figure 5d), suggesting a high therapeutic efficacy. To further assess the changes in CSC phenotype in B16F10-CD44$^+$-bearing mice, the expression of miR-34a-targeted CD44 was examined. A FITC-labeled anti-mouse CD44 antibody was used for immunofluorescence staining of normal and tumoral cells detached from the B16F10-CD44$^+$-bearing lungs. Flow cytometry analysis of CD44 phenotype on the cell surface showed that 38% of cells were CD44-positive in miSLNs-34a-treated lungs, compared to the control groups (PBS: 56%; mock: 71%; miR-34a: 64%; $P<0.05$; Figure 5e). In an immunohistochemisty test, the vast majority of cells in the tumor-bearing lungs were strongly CD44 positive when treated with PBS, mock, and miR-34a, while CD44 immunohistochemical patterns in the miSLNs-34a group were opposite (low CD44 level; Figure 5f), thus indicating that miSLNs-34a could inhibit CSC growth by attenuating CD44 expression.

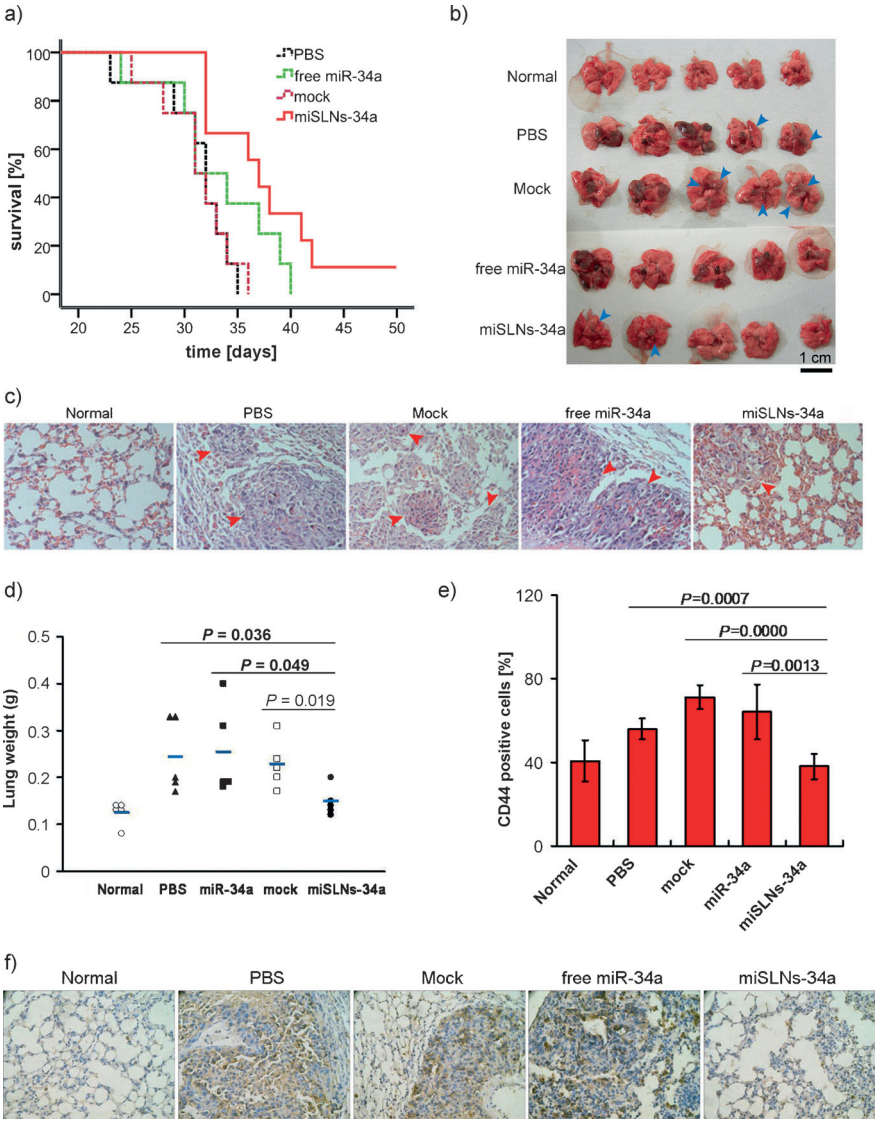

Figure 5. miSLNs-34a inhibition of growth and metastasis of tumors originating from CSCs. a) Survival analysis of B16F10-CD44$^+$-bearing mice ($n=8$). b) Images of the B16F10-CD44$^+$-bearing lungs on the day 21 after three consecutive intravenous injections of miSLNs-34a ($n=5$–6; arrow: tumor nodules). c) Histological staining of the CSC-bearing lungs after miR-34a treatment (arrow: tumor nodules). d) Enhanced antitumor effects of miSLNs-34a evaluated by CSC-bearing lung weight ($n=5$–6). e) Flow cytometric evaluation of CD44 expression in the B16F10-CD44$^+$-bearing lungs after miR-34a treatment. f) Representative CD44 immunohistochemistry images of B16F10-CD44$^+$-bearing lungs after miR-34a treatment.

In general, the therapeutic efficacy of miR-34a depends on its inherent characteristics as well as accessibility of the target site. In this study, we have validated that CSC-like B16F10-bearing lung tumors were significantly inhibited by the miSLNs-34a delivery system, which increases the drug concentration at the target sites because of the enhanced permeability and retention (EPR) effect,[18] while the tumors showed greater resistance to PBS, blank SLNs, and free miR-34a because of the fairly low local concentration of miR-34a in the tumor sites. We also demonstrated that miSLNs-34a effectively delivered miR-34a into the tumor tissue to induce the apoptosis of tumor cells by regulating CD44 expression and the migratory, invasive, and metastatic properties of CSC-like cells. Thus, suppression of CD44 in B16F10-CD44$^+$ cells inhibited tumor development and tumorigenicity (Figure 5), consistent with CD44 possibly playing a role in mediating CSC migration and homing and metastasis.[6]

Toxicity is one of the crucial factors to consider in evaluating the application potential of therapeutic agents.[5] Morphological assessments and tissue histology from H&E

staining of lungs and brains revealed no inflammation and no cellular damage induced by SLNs (Figure S9). We also examined IL-6 concentration in the serum to assess whether inflammatory responses were induced by the nanoparticles. Figure S9b shows that there were no significant changes in IL-6 values detected between untreated and miSLNs-treated groups. These results indicated that miSLNs-34a accumulation occurred in the lung without inducing inflammation, thus suggesting that miSLNs are not toxic under these conditions.

In summary, we have successfully developed a lipid nanoparticle system to carry a microRNA relevant for CSC therapy. MiSLNs protect the integrity of miR-34a from degradation in the serum and increase its cellular-transfection efficiency in vitro. Consequently, this formulation could induce B16F10-CD44$^+$ cell apoptosis and inhibit cell migration by negatively regulating the cell surface protein CD44. Additionally, miSLNs enable miR-34a accumulation in lungs in vivo, extending the persistence of drug in the tumor sites based on the EPR effect. MiSLNs-34a was also effective in inhibiting B16F10-CD44$^+$ tumor development and tumorigenicity with an adequate margin of safety in vivo. Taken together, the potency of miSLNs-34a against CSC-like cells both in vitro and in vivo highlights that we have achieved a viable nanoparticulate delivery system for miR-34a for lung CSC therapy.

Received: October 8, 2012
Revised: December 30, 2012
Published online: February 28, 2013

Keywords: cancer stem cells · drug delivery · microRNA · solid lipid nanoparticles

[1] J. A. Leal, A. Feliciano, M. E. Lleonart, *Med. Res. Rev.* **2013**, *33*, 112 – 138.
[2] S. H. Choi, S. E. Jin, M. K. Lee, S. J. Lim, J. S. Park, B. G. Kim, W. S. Ahn, C. K. Kim, *Eur. J. Pharm. Biopharm.* **2008**, *68*, 545 – 554.
[3] X. Wu, H. Chen, X. Wang, *Cancer Treat. Rev.* **2012**, *38*, 580 – 588.
[4] T. Klonisch, E. Wiechec, S. Hombach-Klonisch, S. R. Ande, S. Wesselborg, K. Schulze-Osthoff, M. Los, *Trends Mol. Med.* **2008**, *14*, 450 – 460.
[5] Y. Chen, X. Zhu, X. Zhang, B. Liu, L. Huang, *Mol. Ther.* **2010**, *18*, 1650 – 1656.
[6] C. Liu, K. Kelnar, B. Liu, X. Chen, C. D. Davis, H. Li, L. Patrawala, H. Yan, C. Jeter, S. Honorio, et al., *Nat. Med.* **2011**, *17*, 211 – 215.
[7] S. J. Lee, M. S. Huh, S. Y. Lee, S. Min, S. Lee, H. Koo, J. Chu, K. E. Lee, H. Jeon, Y. Choi, K. Choi, Y. Byun, S. Y. Jeong, K. Park, K. Kim, I. C. Kwon, *Angew. Chem.* **2012**, *124*, 7315 – 7319; *Angew. Chem. Int. Ed.* **2012**, *51*, 7203 – 7207.
[8] a) S. J. Shi, Z. R. Zhong, J. Liu, Z. R. Zhang, X. Sun, T. Gong, *Pharm. Res.* **2012**, *29*, 97 – 109; b) T. Helgason, T. S. Awad, K. Kristbergsson, D. J. McClement, J. Weiss, *J. Colloid Interface Sci.* **2009**, *334*, 75 – 81; c) J. Jin, K. H. Bae, H. Yang, S. J. Lee, H. Kim, Y. Kim, K. M. Joo, S. W. Seo, T. G. Park, D. H. Nam, *Bioconjugate Chem.* **2011**, *22*, 2568 – 2572; d) A. P. del Pozo-Rodríguez, D. Delgado, M. A. Solinis, A. R. Gascon, J. L. Pedraz, *Int. J. Pharm.* **2007**, *339*, 261 – 268; e) E. Vighi, E. Leo, *Nanomedicine* **2012**, *7*, 9 – 12.
[9] a) C. E. Thomas, A. Ehrhardt, M. A. Kay, *Nat. Rev. Genet.* **2003**, *4*, 346 – 358; b) K. Choi, S. H. Choi, H. Jeon, I. S. Kim, H. J. Ahn, *ACS Nano* **2011**, *5*, 8690 – 8699.
[10] M. D. Joshi, R. H. Müller, *Eur. J. Pharm. Biopharm.* **2009**, *71*, 161 – 172.
[11] R. Li, J. S. Eun, M. K. Lee, *Arch. Pharmacal Res.* **2011**, *34*, 331 – 337.
[12] S. Mizuarai, K. Ono, J. You, M. Kamihira, S. Iijima, *J. Biochem.* **2001**, *129*, 125 – 132.
[13] N. Balekar, N. G. Katkam, T. Nakpheng, K. Jehtae, T. Srichana, *J. Ethnopharmacol.* **2012**, *141*, 817 – 824.
[14] a) D. Beier, P. Hau, M. Proescholdt, A. Lohmeier, J. Wischhusen, P. J. Oefner, L. Aigner, A. Brawanski, U. Bogdahn, C. P. Beier, *Cancer Res.* **2007**, *67*, 4010 – 4015; b) S. Takaishi, T. Okumura, S. Tu, S. S. W. Wang, W. Shibata, R. Vigneshwaran, S. A. K. Gordon, Y. Shimada, T. C. Wang, *Stem Cells* **2009**, *27*, 1006 – 1020.
[15] L. Jin, K. J. Hope, Q. Zhai, F. Joffe, J. E. Dick, *Nat. Med.* **2006**, *12*, 1167 – 1174.
[16] I. Texier, M. Goutayer, A. D. Silva, L. Guyon, N. Djaker, *J. Biomed. Opt.* **2009**, *14*, 054005.
[17] Y. Wu, M. Crawford, B. Yu, Y. Mao, S. P. Sinkam, L. J. Lee, *Mol. Pharm.* **2011**, *8*, 1381 – 1389.
[18] L. Li, Y. Guan, H. Liu, N. Hao, T. Liu, X. Meng, C. Fu, Y. Li, Q. Qu, Y. Zhang, et al., *ACS Nano* **2011**, *5*, 7462 – 7470.

